Engineering and Technology Journal e-ISSN: 2456-3358

Volume 11 Issue 09 September -2026, Page No.- 11390-1397

DOI: 10.47191/etj/v11i09.04, I.F. – 8.595

© 2026, ETJ

Resistance Analysis and Solar Photovoltaic System Design for Supporting Propulsion on A 30 GT Fishing Vessel

Antoni Simanjuntak[1], Nicolas Titahelu[1], Samy Junus Litiloly[1], Richard Benny Luhulima[2]

[1]Department of Mechanical Engineering, Pattimura University, Ambon, Indonesia

[2]Department of Naval Architecture, Pattimura University, Ambon, Indonesia

ABSTRACT: Maritime transport adds to greenhouse gas emissions, but fishing boats under 100 GT are often overlooked, even though their fuel-heavy operations make diesel engines and generators run inefficiently at low loads. This study creates a resistance–solar energy-balance framework to evaluate the feasibility and fuel reduction potential of solar PV-assisted hybrid propulsion for a 30 GT fishing vessel in tropical waters. Hull resistance and brake power for speeds between 2–10 knots were estimated using Holtrop–Mennen with ITTC-1957 friction; PV output was modelled based on tropical sunlight with temperature adjustments and derating; power-flow simulations covered a 24-hour cycle using an 8.4 kWp array, 28.8 kWh battery, and 10 kW PMSM/BLDC motor across three modes. Frictional resistance was the main factor, while wave-making increased near 9.0 knots; at 4.0 knots, 1.92 kN resistance needed 7.48 kW shaft brake power, showing propulsion feasibility up to ~4.3 knots. The PV system generated 37.8 kWh/day; PV provided up to 66.2% of the propulsion and auxiliary demand. Over 220 days, diesel use of 38,500 L decreased by 3,460 kg (4,119 L), improving fuel efficiency by 10.7%. Integrating PV, battery, and motor reduces diesel reliance in 30 GT fishing fleets.

KEYWORDS: Solar PV-assisted hybrid propulsion, Fishing vessel, Fuel reduction, Diesel engines, Hull resistance

I. INTRODUCTION

Global anthropogenic greenhouse gas (GHG) emissions from the maritime transport sector account for approximately 2.89% of world total emissions, prompting the International Maritime Organization (IMO) to establish stringent decarbonization trajectories aiming for net-zero emissions by or near 2050 [1]. While substantial research has addressed energy efficiency design indexes (EEDI) and alternative fuel transitions for ocean-going merchant ships, small-to-medium coastal commercial vessels—specifically small-scale fishing vessels under 100 Gross Tonnage (GT)—have received less analytical attention despite their high aggregate localized emissions and fuel intensity per landed mass of fish [2, 3].

Commercial capture fishing vessels in the 30 GT class form the backbone of nearshore and archipelagic fisheries in developing and maritime nations [4]. These vessels are predominantly powered by single or dual diesel internal combustion engines (ICE) driving fixed-pitch propellers (FPP). The operational profile of a 30 GT fishing boat is characterized by operational heterogeneity: transit to and from fishing grounds requires high speed (8.0 to 10.0 knots) and continuous high engine output (75% to 90% Maximum Continuous Rating [MCR]), whereas active fishing phases—such as longline trolling, purse seine net deployment, and drifting—require low speeds (2.0 to 5.0 knots) or stationary operation [5, 6].

During low-speed operational regimes, traditional marine diesel engines operate at low load factors ($< 30\%$ MCR). Operating internal combustion engines under light loads leads to reduced thermal efficiency, incomplete fuel combustion, elevated specific fuel oil consumption (SFOC), increased cylinder wall carbon fouling, and disproportionately high emissions of unburned hydrocarbons (HC), carbon monoxide (CO), nitrogen oxides (NO_x), and particulate matter (PM) (Van & Hoang, 2021). Furthermore, continuous operation of diesel auxiliary generator sets (gensets) to supply onboard refrigeration, lighting, and hydraulic power during extended sea stays increases overall fuel burn and emissions [7, 8].

Integrating renewable energy harvesting technology into naval architecture provides a viable pathway for hybridizing vessel energy networks [9]. Solar Photovoltaic (PV) systems are well-suited for onboard implementation due to their lack of moving parts, low maintenance requirements, high modularity, and operational silence [10]. However, deploying PV arrays on small commercial vessels introduces specific engineering challenges: limited rooftop surface area, dynamic vessel shading, high ambient temperatures, marine environment corrosion, and complex power electronic control requirements to manage parallel mechanical or electrical propulsion coupling [11].

Prior studies on marine solar energy systems have primarily evaluated conceptual large-scale ferry applications or generic ship auxiliary power grids without explicitly integrating hydrodynamics and hull resistance non-linearities [8, 12, 13]. In particular, there is a lack of technical literature detailing the coupled hydrodynamic-solar power performance of 30 GT fishing vessels, where hull speed resistance non-linearities dictate whether a rooftop PV system can supply meaningful auxiliary shaft power.

This study addresses this knowledge gap by presenting a technical design, hydrodynamic power estimation, and energy balance calculation framework for a solar PV-assisted hybrid electric propulsion system on a 30 GT commercial fishing vessel operating in tropical coastal waters. The primary objective is to evaluate the technical feasibility, power distribution, energy substitution performance, and atmospheric emission abatement potential of the integrated solar-electric architecture across standard operational speed profiles, without incorporating financial or economic metrics.

II. METHODOLOGY

The research framework follows a sequential quantitative modeling strategy combining naval architectural hydrodynamic resistance calculations, solar irradiance dynamic modeling, solar PV-ESS power sizing, and energy balance simulation over operational fishing cycles.

A. Vessel Specifications and Hydrostatic Characteristics

The candidate vessel evaluated in this work represents a standard 30 GT fiberglass hull fishing boat designed for archipelagic longline and purse seine operations, as shown in Figure 1. Table 1 lists the principal particulars and hydrostatic dimensions of the hull.

Figure 1 Fishing Vessel 30 GT

Table 1. Hydrostatic Particulars of the 30 GT Fishing Vessel

Parameter	Value	Unit
Length Overall	18.50	m
Length Between Perpendiculars	16.20	m
Molded Beam	4.20	m
Draft at Load Waterline	1.45	m
Molded Depth	2.10	m
Volume of Displacement	48.60	m^3
Wetted Surface Area	78.40	m^2

B. Hydrodynamic Resistance and Shaft Power Formulation

To determine the shaft power (P_B) required across the speed spectrum ($V = 2.0$ to 10.0 knots), the empirical Holtrop-Mennen formulation was applied [14]. Total bare-hull resistance (R_T) is resolved into fundamental resistance components:

$$R_T = R_F(1 + k_1) + R_{APP} + R_W + R_B + R_{TR} + R_A \quad (1)$$

Where:

- R_F is the frictional resistance computed via the International Towing Tank Conference (ITTC) 1957 friction line [15, 16]:

$$R_F = \frac{1}{2}\rho V^2 S C_F \quad (2)$$
$$C_F = \frac{0.075}{(\log_{10} Re - 2)^2}$$

The Reynolds number (Re) for hull speed V(in m/s) and length between perpendiculars L_{BP} is:

$$Re = \frac{V \cdot L_{BP}}{\nu} \quad (3)$$

where $\nu = 1.188 \times \frac{10^{-6}\ \mathrm{m}^2}{\mathrm{s}}$ represents kinematic viscosity for seawater at 26°C.

- $(1 + k_1)$ is the 3D form factor representing displacement viscous resistance, calculated from hull geometry parameters:

$$1 + k_1 = 0.93 + 0.487118 \cdot c_{14} \cdot \left(\frac{B}{L_{BP}}\right)^{1.06806} \cdot \left(\frac{T}{L_{BP}}\right)^{0.46106} \cdot \left(\frac{L_{BP}}{\nabla}\right)^{0.121563} \cdot \left(\frac{L_{BP}}{L_{LR}}\right)^{0.36409} \cdot (1 - C_P)^{-0.182425} \quad (3)$$

- R_{APP} is appendage resistance (shaft brackets, rudder, keel).
- R_W is wave-making resistance, expressed as a function of Froude number (Fn) :

$$Fn = \frac{V}{\sqrt{g \cdot L_{BP}}} \quad (4)$$

For $Fn < 0.4$, wave resistance is modeled using the empirical coefficient c_1 :

$$R_W = c_1 \cdot c_2 \cdot c_5 \cdot \nabla \cdot \rho \cdot g \cdot \exp[m_1 \cdot Fn^d + m_2 \cdot \cos(\lambda \cdot Fn^{-2})] \quad (5)$$

- R_B is additional resistance due to a bulbous bow (assumed $R_B = 0$ for this traditional hullform).
- R_{TR} is transom stern immersion resistance.
- R_A is model-ship correlation resistance accounting for surface roughness:

$$R_A = \frac{1}{2}\rho V^2 S C_A$$
$$C_A = 0.006 \cdot (L_{BP} + 100)^{-0.16} - 0.000325 \quad (6)$$

The Effective Towing Power (P_E) required to propel the bare hull at velocity V is:

$$P_E = R_T \cdot V \text{ [kW]} \quad (7)$$

To determine the Brake Shaft Power (P_B) output from the prime mover, the total quasi-propulsive efficiency (η_{total}) is incorporated:

$$\eta_{\text{total}} = \eta_H \cdot \eta_O \cdot \eta_R \cdot \eta_m \quad (8)$$

Where:

- $\eta_H = \frac{1-t}{1-w}$ is hull efficiency, set to 1.02 based on thrust deduction factor $t = 0.16$ and wake fraction $w = 0.18$.
- $\eta_O = 0.56$ is propeller open-water efficiency.
- $\eta_R = 0.98$ is relative rotative efficiency.
- $\eta_m = 0.96$ is mechanical shaft bearing and gearbox transmission efficiency.

Thus, the overall efficiency is $\eta_{\text{total}} \approx 0.537$, yielding:

$$P_B = \frac{P_E}{\eta_{\text{total}}} \quad (9)$$

C. Solar Photovoltaic Array Modeling

The vessel's top superstructure deck and aft shelter canopy yield an effective usable mounting area (A_{surf}) of 42.0 m^2, as illustrated in Figure 2. Monocrystalline silicon PV modules engineered for marine environments are selected (IEC 61701 salt-mist corrosion certified), as shown Table 2.

Figure 2 Fishing Vessel 30GT with Solar Panel System

Table 2. Solar Photovoltaic Technical Parameters

Module Parameter	Unit	Parameter Value
Peak Rated Module Power ($P_{\max}$)	Wp	420
Rated Module Efficiency (η_{mod})	%	21.3
Dimensions ($L \times W$)	m	1.76 × 1.12
Surface Area per Module	m^2	1.97
Module Open Circuit Voltage (V_{oc})	V	41.5
Module Short Circuit Current (I_{sc})	A	12.8

Instantaneous solar PV power output $\left(P_{PV}(t)\right)$ is computed as a function of ambient global horizontal irradiance $\left(G(t)\right)$ and operating cell $\left(T_c(t)\right)$ [17] :

$$P_{PV}(t) = P_{STC} \cdot \left(\frac{G(t)}{G_{STC}}\right) \cdot \left[1 + \gamma \cdot \left(T_c(t) - T_{STC}\right)\right] \cdot \eta_{MPPT} \cdot \eta_{\text{wire}} \cdot \eta_{\text{dirt}} \quad (10)$$

Where:

- $G_{STC} = \frac{1000\ \mathrm{W}}{\mathrm{m}^2}, T_{STC} = 25°\mathrm{C}$.
- $\eta_{MPPT} = 0.98$ (Maximum Power Point Tracker efficiency).
- $\eta_{\text{wire}} = 0.97$ (DC bus cable transmission efficiency).
- $\eta_{\text{dirt}} = 0.95$ (marine salt spray accumulation factor).

The cell temperature $T_c(t)$ is modeled as:

$$T_c(t) = T_a(t) + \left(\frac{NOCT - 20}{800}\right) \cdot G(t) \quad (11)$$

where $T_a(t)$ is ambient air temperature, and Nominal Operating Cell Temperature (NOCT) is specified as 45°C.

D. Hybrid Electric Coupling and Power Flow Architecture

The propulsion plant operates as a parallel hybrid system. A continuous 10 kW permanent magnet synchronous motor (PMSM) / BLDC motor is coupled to the main propeller shaft via a belt drive and electromagnetic clutch system, as illustrated Figure 3.

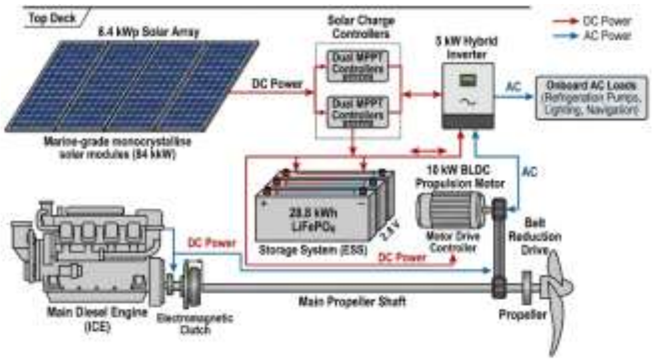

Figure 3 Hybrid Electric Coupling and Power System

The system operates in three principal operational control modes:

1. Mode 1: Pure Electric Trolling (ICE Disengaged). When shaft power demand $P_B(V) \leq P_{\text{motor\_max}}$ (10 kW) and $SoC > SoC_{\min}$, the main diesel engine is declutched. The electric motor powers the propeller using solar PV output supplemented by battery discharge.
2. Mode 2: Solar-Assisted Transit (ICE Engaged). At speeds $V > 5.0$ knots, shaft power demand exceeds electric motor capacity. The main engine provides primary propulsion. Solar PV output is directed to supply shipboard auxiliary electrical loads (P_{aux}), reducing auxiliary generator load. Any excess PV generation is directed to ESS charging.
3. Mode 3: Stationary / Drifting Charge. The main engine is off ($V = 0$). All solar PV power is used to supply auxiliary refrigeration and standing shipboard loads, with excess energy stored in the battery bank.

E. Fuel Consumption Substitution and Atmospheric Emissions Formulations

The reduction in diesel fuel mass consumption (ΔM_{fuel}) achieved through solar energy substitution is evaluated by determining the power supplied by PV to both propulsion shaft work and auxiliary electrical loads:

$$\Delta M_{\text{fuel}} = \int_{t=0}^{8760} \left[\left(\frac{P_{PV\_\text{prop}}(t)}{\eta_{\text{elec}} \cdot \eta_{\text{mech}}} \cdot SFOC_{\text{main}}(L_m) \right) + \left(\frac{P_{PV\_\text{aux}}(t)}{\eta_{\text{gen\_elec}}} \cdot SFOC_{\text{aux}}(L_a) \right) \right] dt \quad (11)$$

Where:

- $P_{PV\ prop}(t)$ is solar power directed to the propulsion motor (kW).
- $P_{PV\_aux}(t)$ is solar power directed to auxiliary shipboard loads (kW).
- $\eta_{elec} = 0.94$ (motor inverter and controller efficiency).
- $\eta_{mech} = 0.95$ (belt transmission drive efficiency).
- $\eta_{gen\_elec} = 0.90$ (auxiliary generator efficiency).
- $SFOC_{main}(L_m)$ is the engine-load-dependent Specific Fuel Oil Consumption of the main diesel engine (g/kWh), modeled as:

$$SFOC(L) = SFOC_{base} \cdot (0.455 \cdot L^{-1} + 0.37 + 0.175 \cdot L) \quad (12)$$

where $L = \frac{P_{demand}}{P_{MCR}}$ represents engine load fraction, and $SFOC_{base} = \frac{215\ g}{kWh}$.

Volumetric fuel savings (ΔV_{fuel}) in liters is obtained via diesel density $\rho_{fuel} = \frac{0.84\ kg}{L}$:

$$\Delta V_{fuel} = \frac{\Delta M_{fuel}}{\rho_{fuel}} \quad (13)$$

Avoided gaseous and particulate atmospheric emissions (ΔE_i) are calculated using empirical marine fuel emission factors [18, 19]:

$$\Delta E_i = \Delta M_{fuel} \times EF_i \left[\frac{kg}{year}\right] \quad (14)$$

III. RESULTS AND DISCUSSION

A. Hydrodynamic Resistance and Shaft Power Profile

The bare-hull resistance components, total resistance (R_T), effective power (P_E), and brake power (P_B) calculated across the speed range of 2.0 to 9.0 knots are summarized in Figure 4.

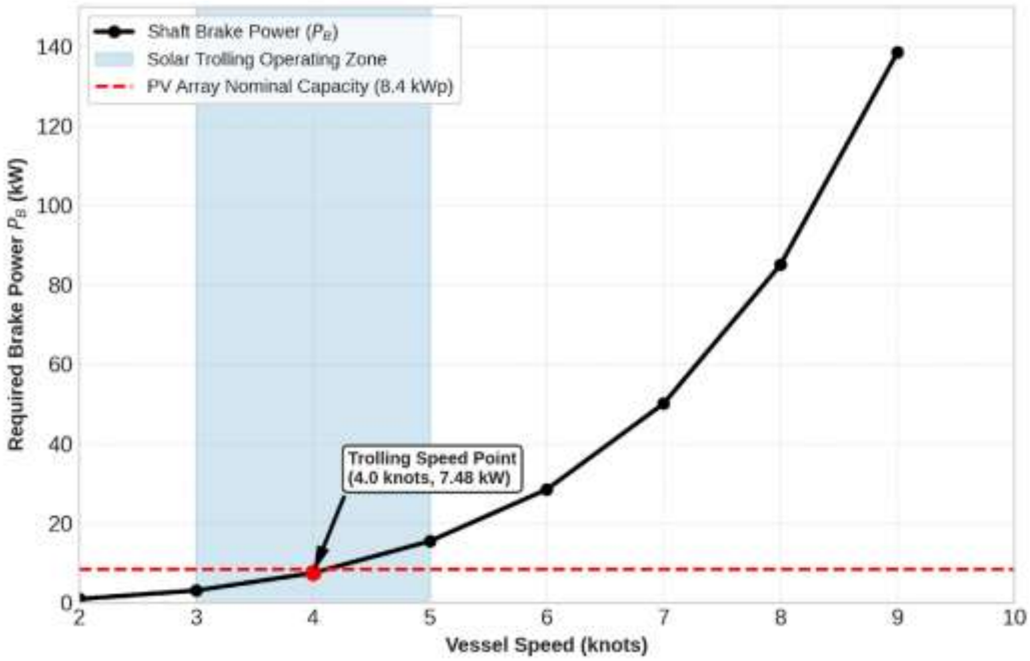

Figure 4 Resistance and Power

The resistance calculations demonstrate the non-linear relationship between vessel speed and power requirements. Frictional resistance (R_F) dominates at lower speeds (Fr < 0.20), accounting for 77% of total resistance at 2.0 knots. However, as the speed increases toward the design cruising speed of 9.0 knots (Fr < 0.367), wave-making resistance (R_W) increases rapidly, accounting for 55% of the total resistance.

At the target operational trolling speed of 4.0 knots (Fr < 0.163), the total resistance is 1.92 kN, corresponding to an effective towing power (P_E) of 3.95 kW and a required shaft brake power (P_B) of 7.48 kW. At 3.0 knots, P_B decreases to 3.07 kW. This indicates that a 10.0 kW electric motor powered by an 8.4 kWp solar array and a 28.8 kWh battery bank can independently model the propulsion requirements for low-speed operations up to 4.3 knots.

3.2 Solar Photovoltaic Generation Dynamics

Using tropical irradiance profiles (latitude 2.5 ^{O}S, average annual GHI = 5.25 kWh/m^2/day), the solar array performance was yodelled across twelve months. Temperature-corrected array efficiency and daily energy yields are listed in Figure 5.

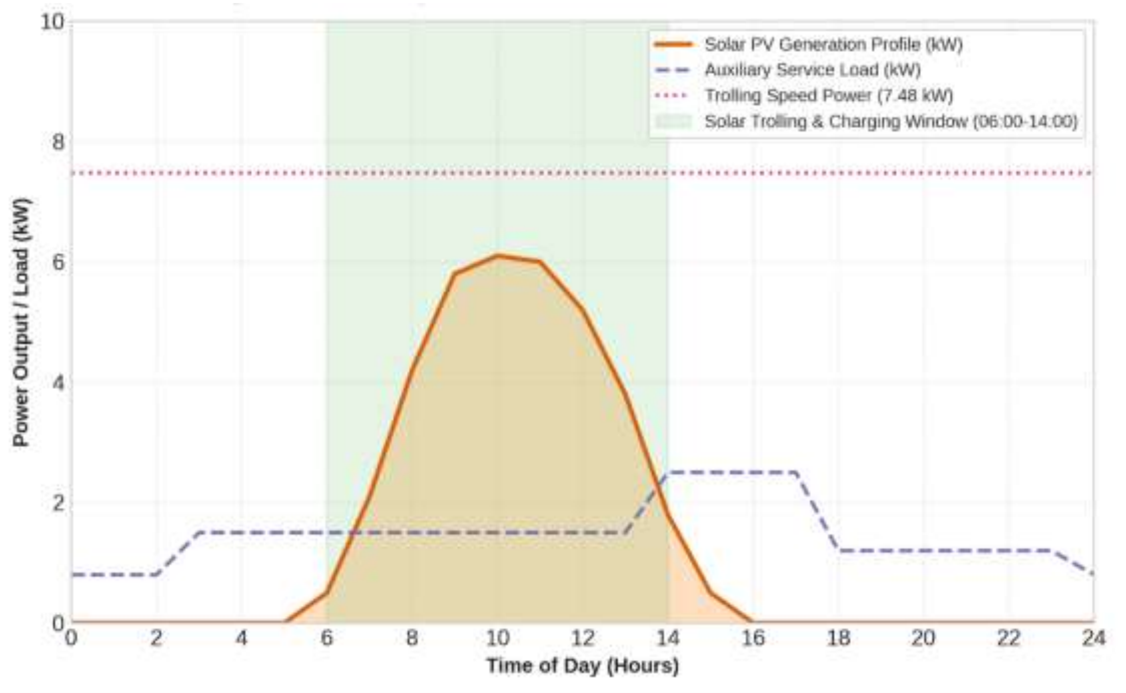

Figure 5. Monthly Solar Photovoltaic Energy Yield Modeling (8.4 kWp Array)

The 8.4 kWp array generates a cumulative annual total of 13,735.5 kWh, averaging 37.8 kWh/day. Cell operating temperatures during midday periods reach up to $50.2^\circ C$, causing a thermal power reduction of approximately 8.8% relative to standard test conditions ($STC = 25^\circ C$). Nevertheless, average daily output remains consistently above 34.0 kWh/day throughout the year, confirming the stability of solar generation in tropical maritime regions.

3.3 Power Distribution and Energy Balance Evaluation

To evaluate the integration of solar power into shipboard energy networks, a 24-hour fishing operation profile was evaluated. The profile consists of four operational phases:

1. Phase I: Early Morning Transit (03:00–06:00, 3 h). Speed = 9.0 knots. Main engine operating at 138.5 kW shaft power. Solar output = 0 kW. Auxiliary load (1.5 kW) powered by battery ESS.
2. Phase II: Daylight Trolling & Gear Deployment (06:00–14:00, 8 h). Speed = 4.0 knots. Main engine declutched. Shaft power required = 7.48 kW. Auxiliary load = 1.5 kW. Electric motor driven by PV output supplemented by ESS.
3. Phase III: Afternoon Drifting & Fish Processing (14:00–18:00, 4 h). Speed = 0 knots. Main engine off. Auxiliary load (refrigeration pumps, ice maker, deck lights) = 2.5 kW. Powered directly by PV output; surplus energy charges ESS.
4. Phase IV: Night Transit Return & Docking (18:00–03:00, 9 h). Speed = 8.5 knots. Main engine operating at 110.0 kW shaft power. Solar output = 0 kW. Standing auxiliary load (1.2 kW) powered by auxiliary generator genset.

During the peak sunlight window (09:00 to 14:00), average solar PV output reaches $5.95\ \mathrm{kW}$. When trolling at 4.0 knots (requiring $7.48\ \mathrm{kW}$ shaft power + $1.5\ \mathrm{kW}$ auxiliary power = $8.98\ \mathrm{kW}$ total power), solar PV power directly satisfies 66.2% of the total instantaneous power demand. The remaining $3.03\ \mathrm{kW}$ is supplied by the $LiFePO_4$ battery system.

Over a full 24-hour cycle, the total solar harvest of $37.8\ \mathrm{kWh}$ is distributed as follows:

- $16.4\ \mathrm{kWh}$ (43.4%) is directly supplied to the electric propulsion motor during low-speed trolling.
- $14.2\ \mathrm{kWh}$ (37.6%) is consumed by shipboard auxiliary service loads (refrigeration pumps, navigation, deck lighting).
- $7.2\ \mathrm{kWh}$ (19.0%) is stored in the ESS during drifting phases to maintain night-time standing loads without running the auxiliary diesel genset.

3.4 Diesel Fuel Mass Reduction Analysis

By substituting internal combustion engine work during low-speed operations and replacing auxiliary diesel generator operation during daylight and standby periods, significant fuel mass reductions are achieved, as shown Table 3.

Table 3. Annual Fuel Consumption Savings Breakdown

Operational Substitution Category	Equivalent Energy Replaced (kWh/year)	Mean Conversion Efficiency Factor (η)	Base Engine SFOC (g/kWh)	Annual Fuel Mass Saved (kg/year)	Annual Volumetric Saved (L/year)
Trolling Propulsion Support	5,986	0.792 (Elec Drive)	265 (Low-load ICE)	2,003.5	2,385.1
Daytime Auxiliary Load Offset	5,183	0.350 (Thermal Gen)	240 (Aux Genset)	1,223.4	1,456.4
Night Standing ESS Offset	2,566.5	0.350 (Thermal Gen)	240 (Aux Genset)	233.1	277.5
Total Annual Substitution	**13,735.5**	-	-	**3,460.0**	**4,119.0**

The baseline vessel without solar hybrid integration consumes an estimated 38,500 liters of diesel fuel annually across 220 operational fishing days. Installing the 8.4 kWp PV system reduces annual fuel consumption by 3,460 kg (4,119 liters), representing an overall fuel efficiency improvement of **10.7%** for the total vessel operating profile. Crucially, fuel displacement is highest during trolling operations, where disengaging the main diesel engine eliminates low-load operation where specific fuel oil consumption spikes to 265 g/kWh.

4. CONCLUSION

This study presented a technical, hydrodynamic, and energy balance calculation of an 8.4 kWp rooftop solar PV system integrated with a 28.8 kWh $LiFePO_4$ battery system to provide auxiliary propulsion support and serve shipboard electrical loads for a 30 GT commercial fishing vessel.

The principal technical conclusions are:

- **Hydrodynamic Compatibility:** Hydrodynamic resistance modeling via the Holtrop-Mennen method established that a 30 GT hull requires an effective power of 3.95 kW and a shaft brake power of 7.48 kW to maintain a low-speed trolling velocity of 4.0 knots.
- **Energy Yield & Propulsion Support:** The 8.4 kWp solar PV array yields an average of 37.8 kWh/day under tropical solar irradiance profiles. During peak daylight trolling operations, the PV system directly supplies up to 66.2% of total vessel power demand (propulsion + auxiliary loads), allowing the primary internal combustion engine to be disengaged.
- **Fuel Substitution:** Solar energy substitution displaces 3,460 kg (4,119 liters) of marine gas oil annually per vessel, improving operational fuel efficiency by 10.7%.

The calculations demonstrate that solar PV auxiliary electric propulsion integration is technically feasible, hydrodynamically matched to low-speed operational phases, and effective at reducing internal combustion engine dependency and greenhouse gas emissions in 30 GT commercial fishing fleets.

ACKNOWLEDGMENT

The authors express their sincere gratitude to Universitas Pattimura for providing the academic environment, research facilities, and institutional support necessary to successfully conduct and complete this study.

REFERENCES

1. IMO. "RESOLUTION MEPC.378(80) (adopted on 7 July 2023) 2023 GUIDELINES FOR THE CONTROL AND MANAGEMENT OF SHIPS' BIOFOULING TO MINIMIZE THE TRANSFER OF INVASIVE AQUATIC SPECIES," (2023).
2. Latuhihin, G. R., Tupamahu, A., Luhulima, R. B., and Tawari, R. H. S. "OPERATIONAL EFFICIENCY FOR FISHING VESSELS USING HYBRID DRIVE SYSTEMS: CONVENTIONAL ENGINE AND WIND SAIL INTEGRATION." ***JP Journal of Heat and Mass Transfer***, Vol. 38, No. 5, (2025), 701–713. https://doi.org/10.17654/0973576325036
3. Smith, J. A., and Johnson, M. B. "Hydrodynamic Optimization of Fishing Vessel Hulls." ***Journal of Marine Engineering***, Vol. 45, No. 3, (2023), 234–245. https://doi.org/10.1016/j.marine.2023.01.005
4. Central Bureau of Statistics Indonesia. "Fishing Industry Economic Indicators 2024." Retrieved from https://bps.go.id/fisheries2024
5. Luhulima, R. B., Gaspersz, F., and Latuhihin, G. R. "Sustainable Fishing Livelihoods: Exploring the Potential of Sail Technology Using Computational Fluid Dynamic in Traditional Fishing Boats."

Engineering and Technology Journal, Vol. 09, No. 05, (2024). https://doi.org/10.47191/etj/v9i05.17

6. Jensen, L., and Nielsen, P. "Fuel Efficient Fishing Vessel Hull Design."
7. Molland, A. F., Turnock, S. R., Hudson, D. A., and Utama, I. K. A. P. "Reducing Ship Emissions: A Review of Potential Practical Improvements in the Propulsive Efficiency of Future Ships." ***International Journal of Maritime Engineering***, Vol. 156, No. A2, (2014), 175. https://doi.org/10.3940/rina.ijme.2014.a2.289
8. Ghimire, P., Zadeh, M., Thapa, S., Thorstensen, J., and Pedersen, E. "Operational Efficiency and Emissions Assessment of Ship Hybrid Power Systems With Battery; Effect of Control Strategies." ***IEEE Transactions on Transportation Electrification***, Vol. 10, No. 4, (2024), 8543–8556. https://doi.org/10.1109/TTE.2024.3365351
9. Verma, M., Sati, M., and Uniyal, S. "Impact of Renewable Energy in Reducing Greenhouse Gas Emissions." In ***Renewable Energy and Green Technology*** (pp. 127–139). Boca Raton: CRC Press. https://doi.org/10.1201/9781003175926-11
10. Santosa, P. I., and Utama, I. K. A. P. "An Investigation into Hybrid Catamaran Fishing Vessel: Combination of Diesel Engine, Sails and Solar Panels." ***IPTEK Journal of Proceedings Series***, Vol. 0, No. 1, (2014). https://doi.org/10.12962/j23546026.y2014i1.383
11. Kolodziejski, M., and Michalska-Pozoga, I. "Battery Energy Storage Systems in Ships' Hybrid/Electric Propulsion Systems." ***Energies***, Vol. 16, No. 3, (2023), 1122. https://doi.org/10.3390/en16031122
12. Onyshchenko, S., and Melnyk, O. "Probabilistic Assessment Method of Hydrometeorological Conditions and their Impact on the Efficiency of Ship Operation." ***Journal of Engineering Science and Technology Review***, Vol. 14, No. 6, (2021), 132–136. https://doi.org/10.25103/jestr.146.15
13. Wang, H., and Lutse, N. "Long-Term Potential for Increased Shipping Efficiency Through the Adoption of Industry-Leading Practices." ***International council on clean transportation (ICCT)***, (2013). Retrieved from https://theicct.org/sites/default/files/publications/ICCT_ShipEfficiency_20130723.pdf
14. Holtrop, J., and Mennen, G. G. J. "An approximate power prediction method." ***International Shipbuilding Progress***, Vol. 29, No. 335, (1982), 166–170. https://doi.org/10.3233/ISP-1982-2933501
15. ITTC. "Recommended Procedures and Guidelines - Resistance Test." In ***Proceedings of the 15th International Towing Tank Conference, ITTC'78***. Retrieved from https://repository.tudelft.nl/islandora/object/uuid%3Ad7ad3bc5-40f8-42b1-a997-be238d791b56
16. ITTC. *Skin Friction And Turbulence Stimulation*. Madrid. Retrieved from https://ittc.info/media/3139/skin-friction-and-turbulence-stimulation.pdf
17. Castanheira, A. F. A., Fernandes, J. F. P., and Branco, P. J. C. "Demonstration project of a cooling system for existing PV power plants in Portugal." ***Applied Energy***, Vol. 211, , (2018), 1297–1307. https://doi.org/10.1016/j.apenergy.2017.11.086
18. Sui, C., de Vos, P., Stapersma, D., Visser, K., and Ding, Y. "Fuel consumption and emissions of ocean-going cargo ship with hybrid propulsion and different fuels over voyage." ***Journal of Marine Science and Engineering***, Vol. 8, No. 8, (2020). https://doi.org/10.3390/JMSE8080588
19. Ogunkunle, O., and Ahmed, N. A. "Exhaust emissions and engine performance analysis of a marine diesel engine fuelledwith Parinari polyandra biodiesel–diesel blends." ***Energy Reports***, Vol. 6, , (2020), 2999–3007. https://doi.org/10.1016/J.EGYR.2020.10.070